D11

THE APPLICATION OF DROPS AND BUBBLES TO THE SCIENCE OF SPACE PROCESSING OF MATERIALS

by

J. R. Carruthers
Bell Laboratories
Murray Hill, New Jersey 07974

I. INTRODUCTION

One of the primary tasks of materials scientists is the preparation of solids with controlled shapes, compositions and structures. These characteristics in turn determine the properties of the solid material. The degree of our ability to exercise control over them ultimately limits the performance of the material for its intended application, whether it be structural, electronic, magnetic, optical, chemical or biological. Consequently studies of materials processing are highly important areas of research which involve interdisciplinary combinations of such diverse fields as solid state physics, surface physics and chemistry, fluid dynamics, heat and mass transfer, and high temperature thermodynamics and physical chemistry. Although there are many important processes such as metals casting and annealing, ceramic sintering, glass melting and homogenization, chemical vapor deposition, crystal growth, oxidation, and diffusion, this paper will consider only crystal growth from melts and solidification processes since these are uniquely affected by a reduced gravity. The basic configurations and problems associated with crystal

growth from melts will be outlined on earth as well as in space. The role of free liquid surfaces in crystal growth processes will be discussed for various liquid shapes and the relevance of the current state of the science of liquid drops and bubbles in liquids to these processes will be demonstrated.

II. CRYSTAL GROWTH AND SOLIDIFICATION PROCESSES ON EARTH

Melt crystal growth techniques can be classified in terms of the degree of confinement of the liquid by an external container as shown in Fig. 1. In the full confinement methods, the growth interface contacts the container over some region as shown for the horizontal and vertical Bridgman techniques.[1] The main problems associated with this contact are direct container contamination of the melt close to the interface itself and the thermal stresses occurring between the container and the grown crystal. In the partial confinement methods, the growth interface does not touch the melt container as shown for the Czochralski, flux and hydrothermal growth techniques.[1] Although contamination from the container does frequently occur in these methods, it can often be reduced through the use of special liners inside the structural support of a rigid container. The Czochralski technique is the most widely used method for growth of congruently melting materials by direct solidification. The growth interface is constrained by appropriate temperature gradients and the meniscus of the

free melt surface. Included here are the shape defining techniques such as the Stepanov method and edge-defined, film-fed method, both of which will be described later. The various flux techniques are basically isothermal and are used for materials that are incongruently melting or decompose at higher temperatures. The interface position and growth rate are constrained by the compositional gradients in the melt and the degree of supersaturation of the melt respectively. For some fluxes, the free surface results in undesirable vaporization of some constituents. Hydrothermal growth produces crystals from a supersaturated fluid near or above its critical temperature. The growth rate is controlled by a concentration gradient induced by a temperature difference between the nutrient and growth regions.

Crystal growth methods from unconfined or containerless melts involve both drops and zones as shown in Fig. 1. Constant volume sessile drops which are fed externally with "raw material" are used for both flux growth by the vapor-liquid-solid (VLS) technique and congruent solidification by the Verneuil technique. Similarly, liquid zones, where the melt surface is constrained by surface tension assisted in some cases by electromagnetic levitation, have been used for both congruent melting (floating zone, silver boat methods) and fluxed melt systems (temperature gradient zone melting or travelling solvent methods). None of these

techniques has been widely used on earth because they are complicated to control and because they require rather high temperature gradients due to the limits imposed on the liquid volume size by hydrostatic pressure considerations. The high temperature gradients cause extensive dislocation generation in the grown crystals and also give rise to highly nonuniform and unstable thermal convection in the melt which in turn leads to undesirable compositional variations in the crystal through its influence on mass transport at the growth interface. The removal of gravitational constraints however leads us to reconsider the detailed behavior of unconfined liquids and the influence of this behavior on crystal growth processes in a later section.

The use of bubbles in materials processing on earth has been mainly as a means of providing large surface areas for gas-liquid reactions in extractive metallurgical processes and for stirring purposes in glassmaking. In reduced gravity environments these techniques cannot be used because it would be difficult to remove the bubbles. On the other hand several novel uses of bubbles in materials processing are possible in reduced gravity which will be discussed in the next section.

III. CRYSTAL GROWTH AND SOLIDIFICATION PROCESSES IN SPACE

Some possible configurations for containerless crystal growth in space are shown in Fig. 2. A division

can be made into single, double and multiple solid access into the liquid drop.

In the single access techniques, the drop is solidified onto a crystal seed so that as the seed is withdrawn, the drop position must be maintained. There are two main techniques for holding the drop position; by external fields such as electromagnetic[2] and stationary acoustic[3,4] fields, and by the use of dies such as used in the Stepanov[5] and edge-defined, film-fed[6,7] techniques. The latter techniques may be used to grow noncircular cross-sectional shapes but reintroduce contamination problems. The use of external positioning fields possesses several complications of which the most important are uncontrolled convection, drop oscillations and what heating method is to be used. In the case of acoustic field positioning, drop oscillations (and associated fluid flow) may be present, optical image heating methods must be used to avoid distortion of the sound fields and the energy impedance mismatch which gives rise to the positioning force becomes weaker in high temperature gases. In the case of electromagnetic field positioning, only liquids with a reasonable electrical conductivity (to 1 mho cm^{-1}) may be used and uncontrolled electromagnetic stirring may be present at higher power levels if the field is used to simultaneously heat as well as position the drop. Both positioning field arrangements will soon be tested in the space environment achievable in sounding rockets.[8]

In all single access drop techniques, control of the meniscus shape at the freezing growth interface will be required for ease of growth-rate and crystal shape control. The role of the meniscus shape will be discussed in the next section but it is desirable that the liquid and solid surfaces meet at an angle of 180°.

The need for positioning fields may be eliminated by the use of double access liquid drop techniques where a melting rod of the same material as the solidifying crystal is introduced into the drop. The simplest concept is the cylindrical floating zone technique[9-11] where the end rods are of equal diameter. In this case, the maximum stable liquid zone length is equal to the circumference regardless of the surface tension.[12] Although this zone length is longer than that possible in earth gravity, a problem arises because the temperature distribution in the absence of thermal convection is not favorable. As shown in Fig. 3(b), the interface shapes will not be perpendicular to the crystal axis as shown in Fig. 2 but will rather follow the freezing point isotherm resulting from thermal conduction. The simplest remedy to this problem will be to use unequal and diameters as typified by the pedestal technique in Fig. 2. This geometry will allow heaters to be used which possess axial as well as radial temperature gradients. If zone lengths longer than the crystal circumference are desired, then floating drop shapes may be used

as shown in Fig. 2. However independent meniscus shape control is not possible for such drop shapes.

Multiple solid access in the liquid drop allows for compositional control of the molten zone during growth. In such a system, complex solid-solution systems could be grown at constant solid composition by continuously changing the liquid composition. However such a technique represents a degree of difficulty not presently attempted on earth with the exception of the feed-in, pull-out and floating crucible techniques.[1]

The role of bubbles in liquid drops has been shown in recent Skylab experiments[13] to effectively "stiffen" the outer liquid surface so that vibrational oscillation amplitudes are considerably diminished. Consequently any of the techniques shown in Fig. 2 may benefit by using liquid shells instead of liquid drops if drop oscillations are a problem.

Another area where bubbles may serve a useful function is in the production of foam solids - a new class of materials with potentially useful strength to weight ratios.

IV. LIQUID DROP STATICS AND DYNAMICS

In this section, we consider four major phenomena relevant to the space processing of molten materials; the degree to which a contained liquid adopts its equilibrium shape in zero gravity, the stable shapes of axisymmetric menisci at crystal-melt boundaries, the rotational stability

of liquid drop and zone surfaces, and the vibration-oscillation characteristics of liquid drops and zones. These phenomena are all basic to our understanding of containerless handling of melts for crystal growth purposes.

(a) Behavior of Confined Liquids at Zero Gravity

There are two important factors which determine the equilibrium shape of a liquid in a container under weightless conditions; the filling factor and the liquid-container contact angle. This problem has been solved analytically for a spherical container by Zenkevich[14] and his results are shown in Fig. 4. The transitions to the various morphological forms are given by the two curves A and B which denote the contact angle, θ, at which the liquid transforms from its earthbound position at an initial height, h, in a container of radius R. Below curve A, the liquid uniformly wets the container while above curve B, the liquid drop does not contact the container at all. A similar set of conditions applies to liquids contained in cylindrical tubes although no analytical solutions are available as yet. These results show that completely confined liquids may adopt a variety of shapes which may not be desirable from the standpoint of crystal growth and solidification, particularly in the vicinity of the transition points of Fig. 4.

(b) Static Meniscus Behavior at Zero Gravity

The behavior of the meniscus shape during Czochralski growth on earth has been discussed thoroughly

by Geist and Grosse.[15] The stabilities of such menisci have been dealt with by Huh and Scriven[16] as well as Padday and Pitts.[17] Basically the situation in Czochralski growth is shown in Fig. 5 where a solid cylinder is immersed in the free liquid-surface at a contact angle of zero. The preferred meniscus height, h_2, is shown in Fig. 5(b) since the freezing interface will tend to remain at constant diameter for small non-uniform displacements of the crystal pulling rate, V_o, or freezing point isotherm. The stabilities of menisci at zero gravity for the free surface, single access drop methods of Fig. 2 have not been investigated as yet but are going to depend quite sensitively on the configurations of the force fields used to constrain the liquid drop position. Some anticipated meniscus shapes at zero gravity are shown in Fig. 6. The maximum height, h, of the crystal interface above the original drop surface is determined primarily by the radial departure, R, allowed at the bottom of the meniscus. If R is constrained to be close to the crystal radius, R_c, then the height h cannot exceed $2\pi R$ without the meniscus becoming unstable. Otherwise longer liquid meniscus columns are allowed according to the approximate relation:

$$h_{max} \approx 2\pi[R^2-(R-R_c)^2]^{1/2} \qquad (1)$$

These considerations apply only if the liquid column base radius, R, is substantially smaller than the liquid drop radius. Otherwise the constant volume condition of the drop or zone will enter into the stability picture as pressure changes in addition to those caused by the liquid surface curvature. A treatment of the mathematical stability of liquid surfaces of revolution under such conditions has been given by Gillette and Dyson[18] for equal end radii. A summary of their calculated stability limits is shown in Fig. 7 for liquid zones of volume V, length L, radius R and diameter D. The limits for unequal end diameters and differential volumes have not been calculated or observed as yet.

(c) Dynamic Behavior of Liquid Surfaces at Zero Gravity

The behavior of free liquid surfaces under rotational and vibrational conditions is now examined.

(i) Rotational Stability

In crystal growth and solidification processes, rotation is usually required in order to provide radially symmetrical temperature distributions since such symmetry may not be present in the heating source and perfect alignment of the crystal axis with the thermal center of symmetry is difficult to achieve. For purposes of compositional homogeneity however, no convection is desired in the melt. Consequently only uniform "solid-body" rotation of the liquid (equal isorotation in the case of double access drop growth

techniques) may be considered and the absolute rotation velocity, ω, must be small enough so that the centrifugal acceleration, $\omega^2 r$, does not cause density gradient driven flows (rotation of a 10 cm radius drop at 5 rpm results in centrifugal accelerations of 2.5×10^{-3} g). Nevertheless such rotations will influence the surface stability criteria discussed in the previous section.

The rotational stability criteria for liquid spheres was first considered by Rayleigh[19] and more completely by Chandrasekhar.[20] The deformed shape considered was that of depression at the poles and expansion at the equator as shown in Fig. 8 for various values of the dimensionless rotation rate, $\rho\Omega^2 R^3/\sigma$ (where ρ is the density and σ the surface tension of the liquid drop of initial radius, R, being rotated at Ω rad/sec). A water drop of radius 10 cm would become toroidal at a rotation rate of 12 rpm. However recent crude experiments performed on Skylab with rotating liquid drops indicated that rather than the expected toroidal deformation shown in Fig. 9(a), a dumb-bell deformation (Fig. 9(b)) was produced when even small nonaxial perturbations are introduced into the rotating drop. The growth rate of such nonaxial perturbations is considerably reduced as the viscosity of the liquid drop increases. Such instabilities have not yet been analyzed theoretically.

The rotational stability criteria for cylindrical liquid columns has been analyzed theoretically by Hocking and Michael[21], Hocking[22], Gillis[23], and Ross[24]. For axisymmetric disturbances, the maximum zone length is reduced below that for a static zone:

$$L_{max} = \frac{2\pi R}{[1+\frac{\rho R^3 \Omega^2}{\sigma}]} \qquad (2)$$

This criterion has been tested experimentally in a Plateau simulation system by Carruthers and Grasso[12] and in real zero gravity on Skylab.[25] These data are summarized in Fig. 10 for equal isorotations and compared to Eq. (2). Discrepancies in the Plateau results occur because the actual zone rotation velocity is somewhat smaller than the end-member rotation velocity because of the viscous drug effects exerted by the viscous outer fluid containing the zone.[2] The Skylab data also shows a deviation from the theoretical curve - becoming unstable at lower rotation rates than expected. The reason for this behavior is that the failure mode in the Skylab experiments was nonaxisymmetric as shown in Fig. 11(b). It was possible to obtain axisymmetric failure modes of the type shown in Fig. 11(a) by replacing the water zone in the Skylab experiments with a soap solution/air foam which greatly increased the effective viscosity. The nonaxisymmetric failures clearly arise from disturbances created by misalignment of the rotation axes and nonparallelism of the discs at the ends of the zone. However viscosity

plays a very important and unsuspected role in determining which types of disturbances are amplified. A great deal of theoretical work is required here to analyze the nonaxisymmetric failure modes for both rotating liquid spheres and cylinder.

(ii) Vibrational Behavior of Free Liquid Surfaces

In crystal growth processes, the time dependent deformation of free liquid surfaces is undesirable because the meniscus shape at the freezing interface will change so as to cause crystal diameter perturbations and also because internal fluid flows will develop which influence the growth segregation behavior. There are two separate liquid shapes which can be considered here as was done for rotational behavior; spherical drops and cylindrical zones. We are interested in the natural resonant oscillation frequencies, which depend primarily on surface tension, and the decay rates, which depend mostly on viscosity. Knowledge of this behavior will permit apparatus designers to avoid vibrations which cause resonant, large amplitude oscillations in the liquid volumes used in space processing.

Lamb first calculated the oscillation frequencies of spherical liquid drops by assuming the viscosity was zero as:[26]

$$\beta^* = \left[\frac{\sigma \ell (\ell+1)(\ell-1)(\ell+2)}{R^3(\rho_o \ell + \rho_i(\ell+1))}\right]^{1/2} \qquad (3)$$

where ℓ is an integer greater than unity and ρ_o and ρ_i are the densities of the fluids outside and inside the drop respectively. The role of viscosity was determined analytically by Miller and Scriven[27] who found that the time dependent frequency, β, varied according to:

$$\beta = \beta_R + i\,\beta_I \tag{4}$$

where β_I is the oscillation frequency and β_R the decay rate and both are viscosity dependent:

$$\beta_R = \frac{(2\ \ell+1)^2(\beta^*\mu_i\mu_o\rho_i\rho_o)^{1/2}}{2\sqrt{2}\ R\Gamma[(\mu_i\rho_i)^{1/2}+(\mu_o\rho_o)^{1/2}]}$$

$$+ \frac{(2\ \ell+1)[2(\ell^2-1)\mu_i^2\rho_i+2\ \ell(\ell+2)\mu_o^2\rho_o+\mu_o\mu_i(\rho_i(\ell+2)-\rho_o(\ell-1))]}{2\ R^2\Gamma[(\mu_i\rho_i)^{1/2}+(\mu_o\rho_o)^{1/2}]^2} \tag{5}$$

$$\beta_I = \beta^* - \frac{(2\ \ell+1)^2(\beta^*\mu_o\mu_o\rho_i\rho_o)^{1/2}}{2\sqrt{2}\ R\Gamma[(\mu_i\rho_i)^{1/2}+(\mu_o\rho_o)^{1/2}]} \tag{6}$$

Here μ_i and μ_o are the dynamic viscosities of the inner and outer fluids respectively and

$$\Gamma = \rho_o\ell + \rho_i(\ell+1) \tag{7}$$

Experimental verification of these relationships can be found in the Plateau simulation work of Valentine et. al.[28] where drops of a carbon tetrachloride and benzene solution with a density of 1 gm cm^{-3} were suspended in water

and oscillated by coalescense with small cyclohexanol drops. More recent experiments[29] using sessile drops of the same organic solution suspended in water are shown in Fig. 12. The drops were deployed by simply filling a glass laboratory funnel so as to obtain the desired size (Fig. 12(a) and (c)) and then mechanically vibrated (Fig. 12(b) and (d)). The data are plotted in Fig. 13 and show that although the decay rates agree well with Eq. (5), the oscillation frequencies appear to lie between β^* and β_I. The contact of the carbon tetrachloride/benzene drop to the glass tube may be responsible for this discrepancy although the contact angle is 130° so that the drop does not wet tube itself.

More recent experimental data has been obtained with liquid drop experiments performed for the author on Skylab mission IV by scientist-astronaut E. Gibson. In these experiments sessile water drops were deployed on a circular disc which was then oscillated along an axis perpendicular to its face. The data are shown on Fig. 14 together with the theoretical predictions of Eqs. (3) and (5). One free drop experiment performed by astronaut W. Pogue on the same mission is included for comparison. In all cases, agreement with theory is excellent for both free and sessile drops.

The vibration behavior of cylindrical liquid zones was also studied extensively on Skylab IV. Preliminary data for the oscillation frequency of longitudinal modes

(vibration along the zone axis) are shown in Fig. 15 together with the theoretical prediction (solid curves) by Lamb[26] for an inviscid fluid:

$$\beta_\ell = \left[\frac{2\ \pi \ell^3 \sigma}{L^3 \rho}\right]^{1/2} \tag{8}$$

where L is the zone length. The frequency increase at longer zone lengths is not presently understood but may be a result of the viscous flow effects in the zone. The theoretical vibration analysis for zones should be redone including these effects as was done for spherical liquid drops (Figs. 13 and 14).

V. SUMMARY

The unique environment of space allows the containerless handling of melts to be used for controlled crystal growth and solidification processes. Some of the techniques currently used on earth together with their problems have been reviewed. Possible configurations for containerless methods in a space environment have been discussed. Such techniques require a detailed understanding of the behavior of free liquid surfaces under both static and dynamic conditions. The current state of knowledge in the science of liquid drops and bubbles relevant to containerless processing has been discussed together with the results of recent Plateau simulation and Skylab experiments. Many areas which require further theoretical and experimental work have been identified as a result of this preliminary work.

REFERENCES

1. See for example - J. C. Brice, The Growth of Crystals from Liquids, Elsevier, New York 1973.
2. R. T. Frost, Proc. Third Space Processing Symposium: Skylab Results, NASA, 1974.
3. T. Wang, ibid.
4. R. Whymark, ibid.
5. A. V. Stepanov, Bull. Acad. Sci. U.S.S.R. 33, 1775 (1969).
6. H. E. LaBelle and A. I. Mlavsky, Mat. Res. Bull. 6, 571-580 (1971).
7. H. E. LaBelle, Mat. Res. Bull. 6, 581 (1971).
8. NASA Sounding Rocket Program, Marshall Space Flight Center, Huntsville, Alabama.
9. P. H. Keck and M. J. E. Golay, Phys. Rev. 89, 1297 (1953).
10. R. Emeis, Z. Naturforsch. 9a, 67 (1954).
11. H. C. Theuerer, Trans. AIME 206, 1316 (1956).
12. J. R. Carruthers and M. Grasso, J. Appl. Phys. 43, 436 (1972).
13. T. C. Bannister, to be published.
14. V. B. Zenkevich, High Temp. 2, 203 (1964).
15. D. Giest and P. Grosse, Z. Angew. Phys. 14, 105 (1962).
16. C. Huh and L. Scriven, J. Coll. Interface Sci. 30, 323 (1969).
17. J. F. Padday and A. R. Pitt, Phil. Trans. Roy. Soc. (London) 275, 489 (1973).
18. R. D. Gillette and D. C. Dyson, Chem. Eng. J. 2, 44 (1971).
19. Lord Rayleigh, Phil. Mag. 28, 161 (1914).

20. S. Chandrasekhar, Proc. Roy. Soc. London A286, 1 (1965).

21. L. M. Hocking and D. H. Michael, Mathematika, 6, 25 (1959).

22. L. M. Hocking, Mathematika, 7, 1 (1960).

23. J. Gillis, Proc. Camb. Phil. Soc. 57, 152 (1961).

24. D. K. Ross, Z. Angew. Math and Phys. 21, 137 (1970).

25. J. R. Carruthers, Proc. Third Space Processing Symposium: Skylab Results, NASA, 1974.

26. H. Lamb, Hydrodynamics, sixth edition, Cambridge University Press, reprinted by Dover, New York 1945.

27. C. A. Miller and L. E. Scriven, J. Fluid Mech. 32, 417 (1968).

28. R. S. Valentine, N. F. Sather and W. J. Heideger, Chem. Eng. Sci. 20, 719 (1965).

29. J. R. Carruthers, unpublished work.

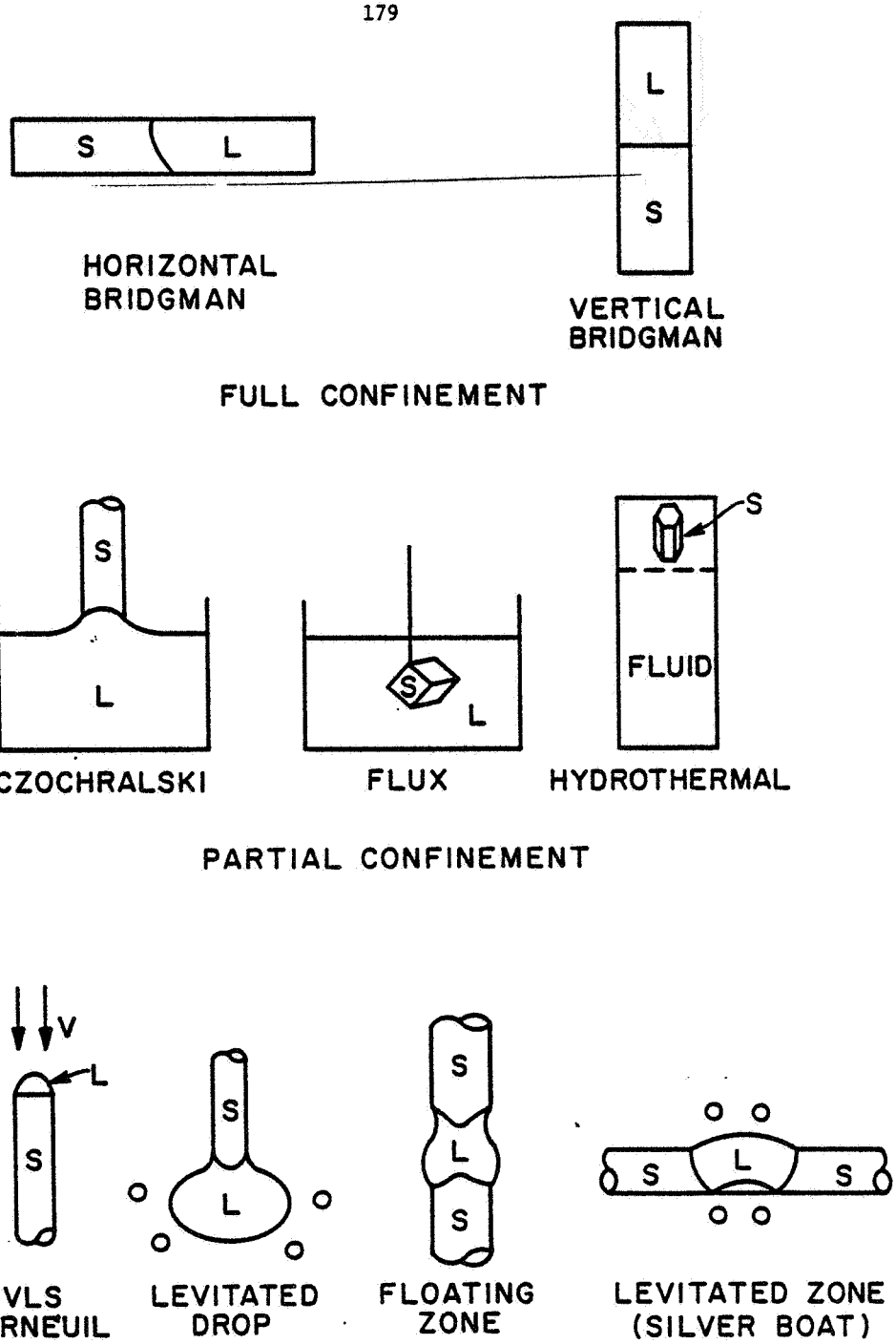

Fig. 1. Schematic classification of melt crystal growth processes on earth in terms of the degree of liquid confinement by a container.

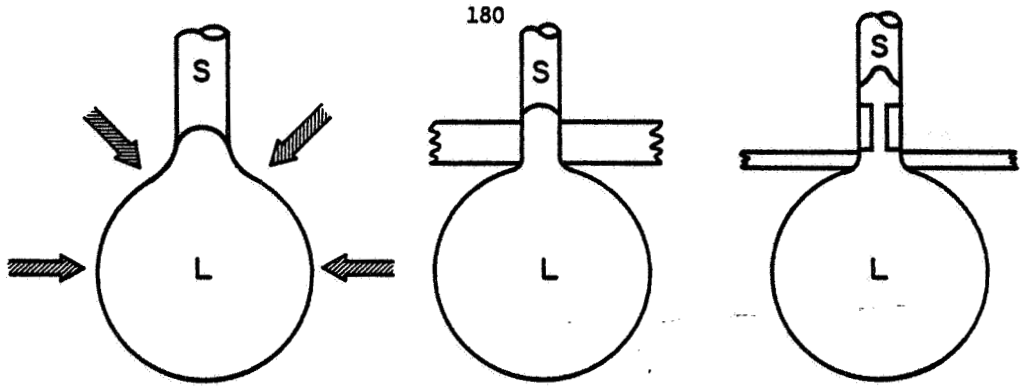

CZOCHRALSKI STEPANOV EDGE-DEFINED FILM-FED

SINGLE ACCESS DROP TECHNIQUES

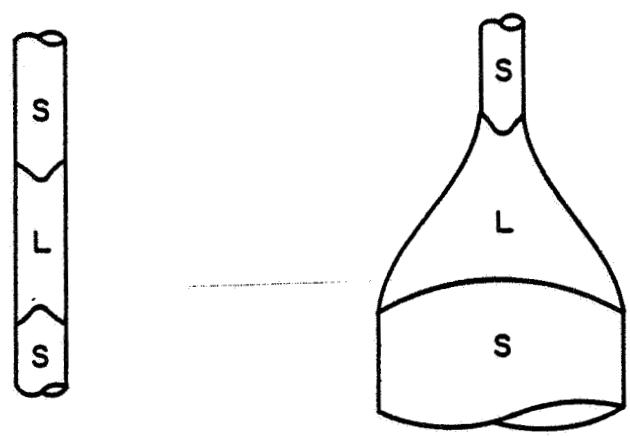

FLOATING ZONE PEDESTAL

DOUBLE ACCESS DROP TECHNIQUES

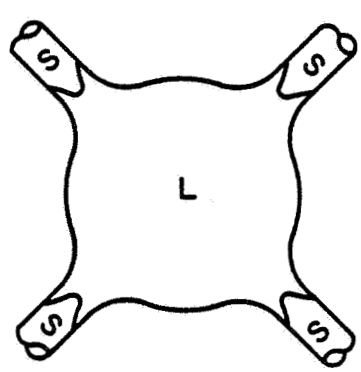

MULTIPLE ACCESS DROP TECHNIQUES

Fig. 2.
Schematic classification of melt crystal growth techniques in space in terms of solid access to the liquid drop.

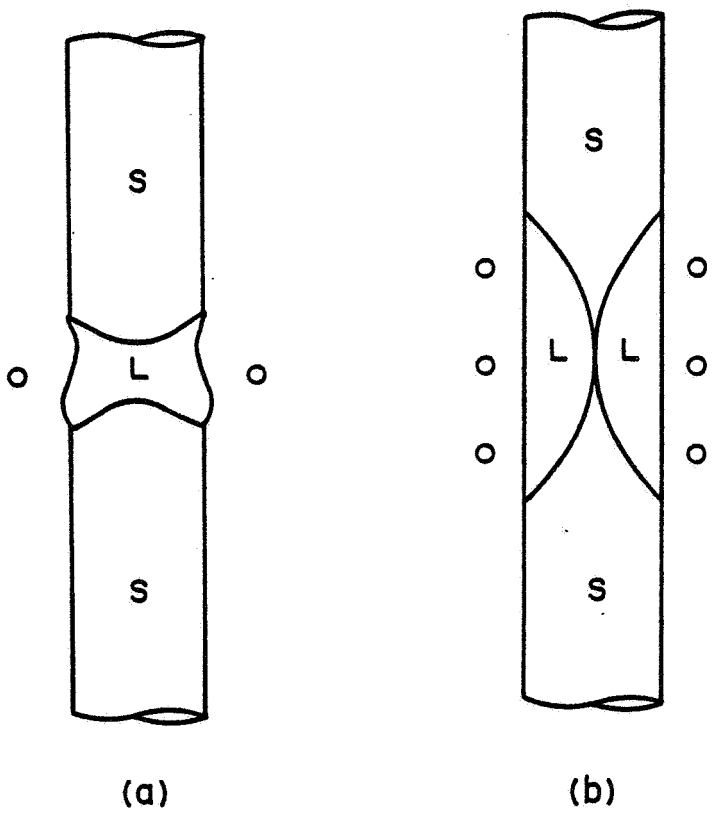

Fig. 3. Crystal-melt interface profiles in zones for (a) earth gravity with thermal convection in the melt and (b) zero gravity with only thermal conduction occurring in the melt.

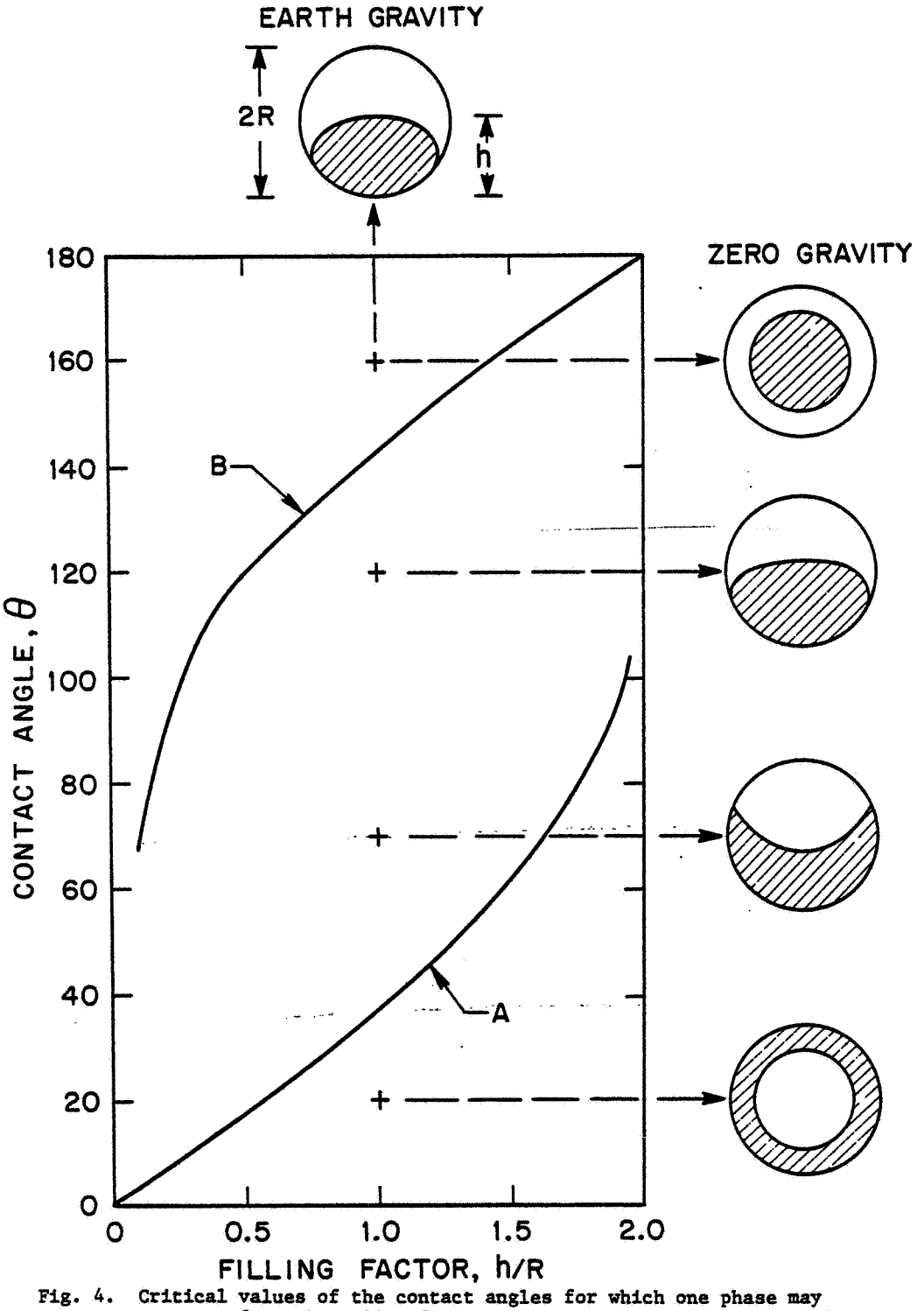

Fig. 4. Critical values of the contact angles for which one phase may separate from the walls of a spherical container at zero gravity. Below curve A, the liquid uniformly coats the walls and above curve B the gas phase uniformly coats the walls - from Zenkevich.(14)

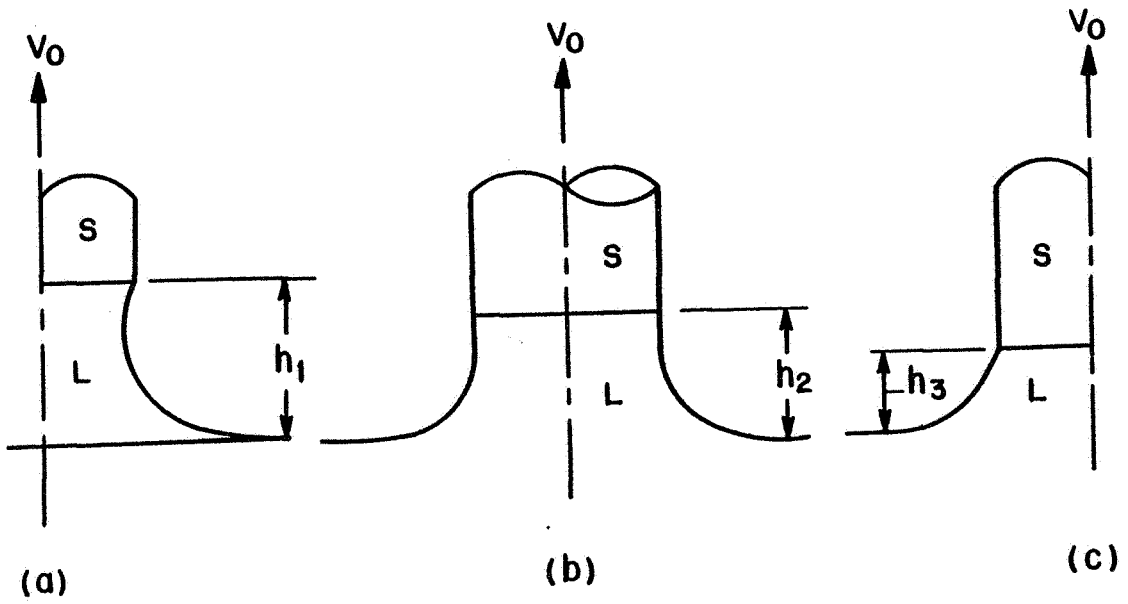

Fig. 5. Menicus configurations important at the crystalmelt interface during Czochralski growth on earth; (a) necking instability, (b) desired configuration, (c) crystal diameter control difficult.

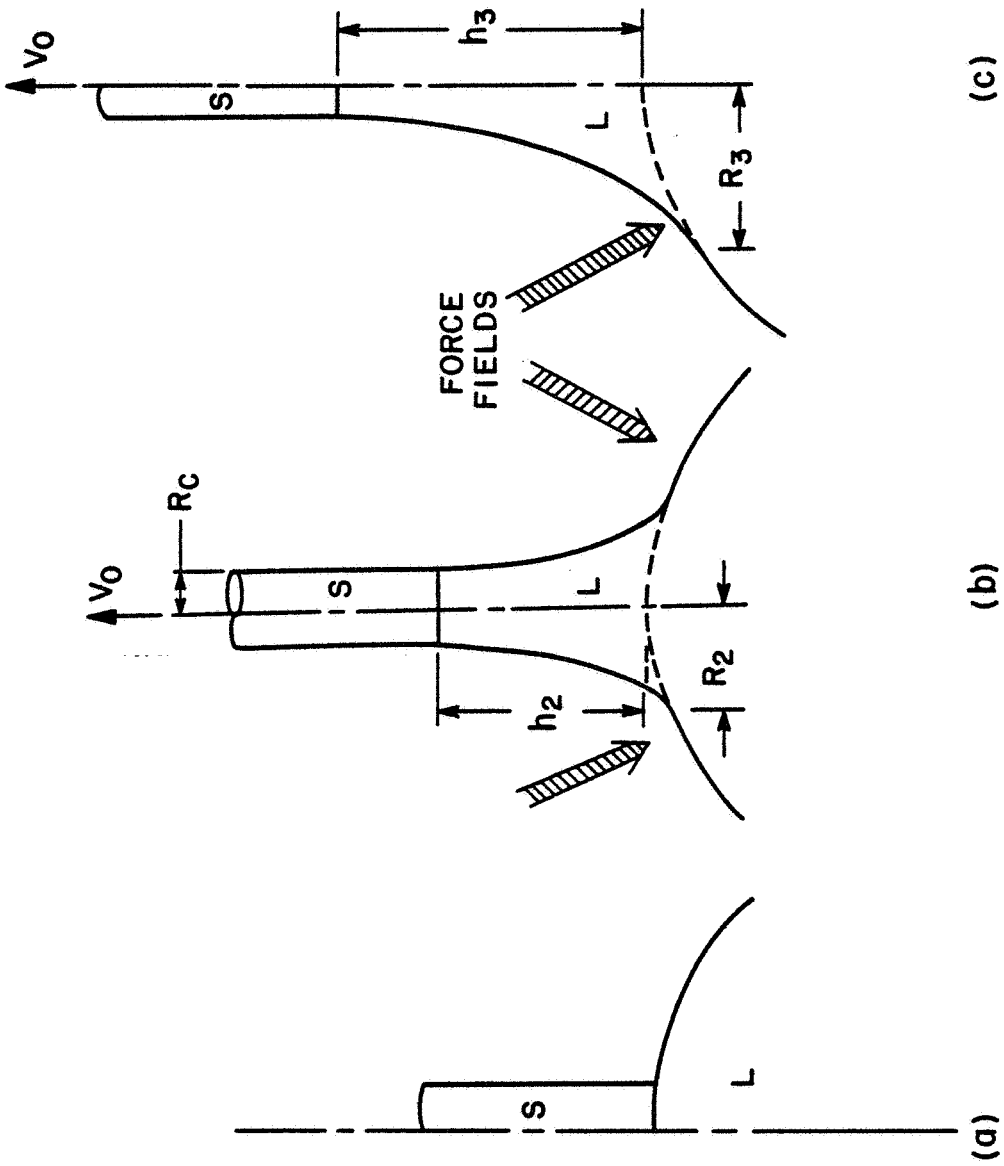

Fig. 6. Menicus configurations for single access liquid drop crystal growth technique of Fig. 2.

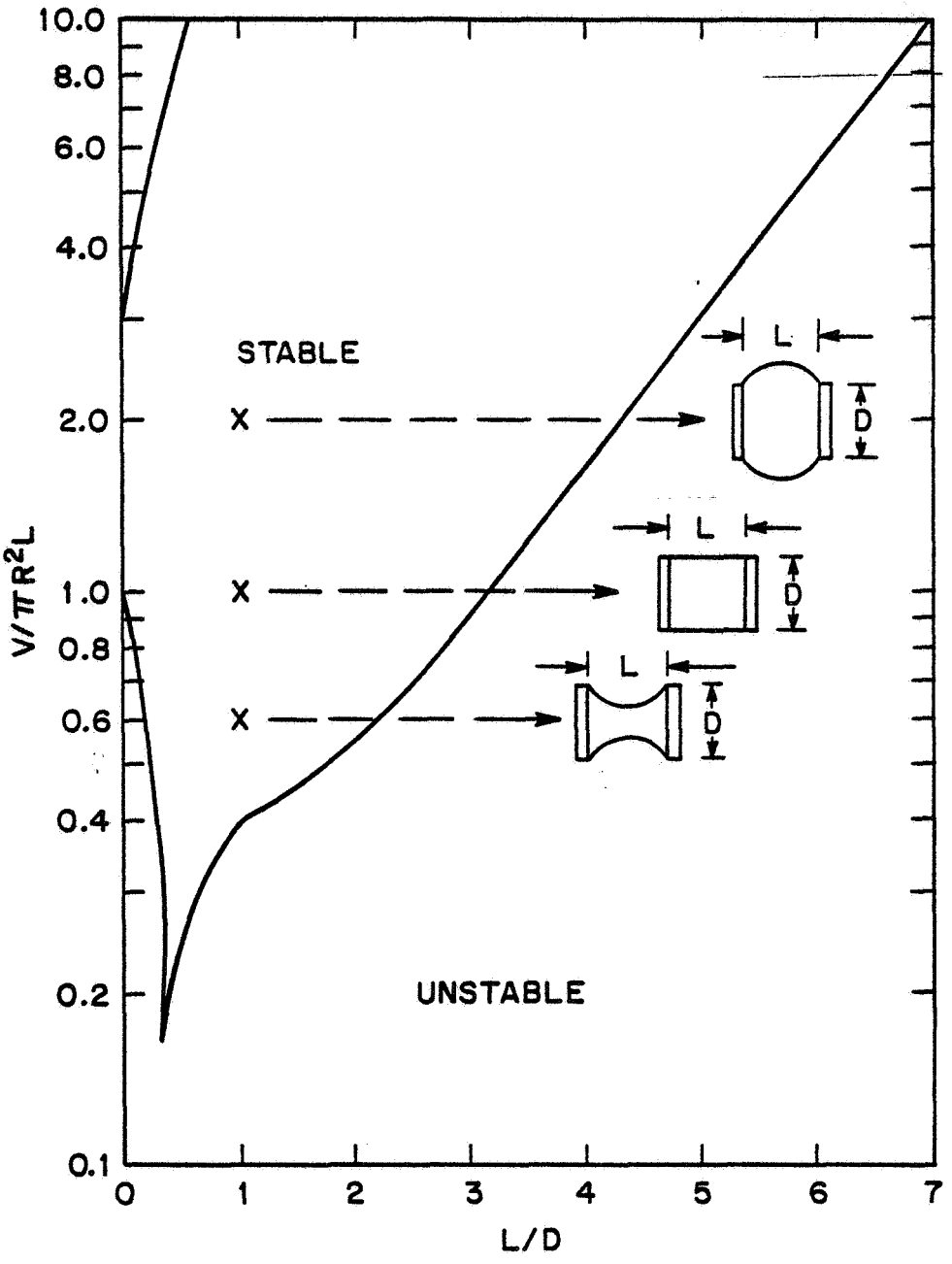

Fig. 7. Stability region of the surface of cylindrical liquid zones of various shapes contained between equal diameter end discs - from Gillette and Dyson.(18)

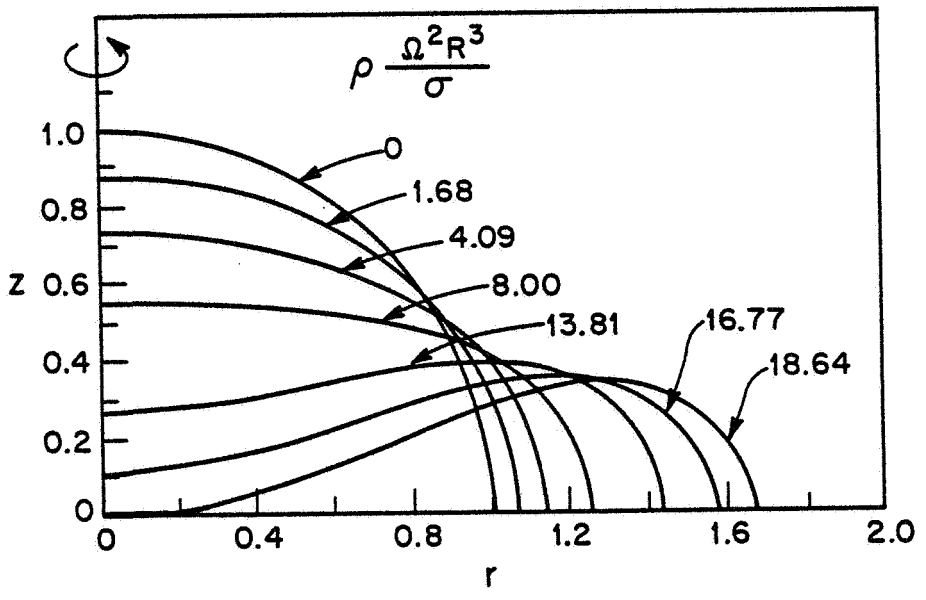

Fig. 8. Calculated shape deformations of an initially spherical liquid drop of radius, R, rotating at increasingly fast rotation rates. Rotation axis is the z-axis and r is the equatorial radius - from Chandrasekhar.

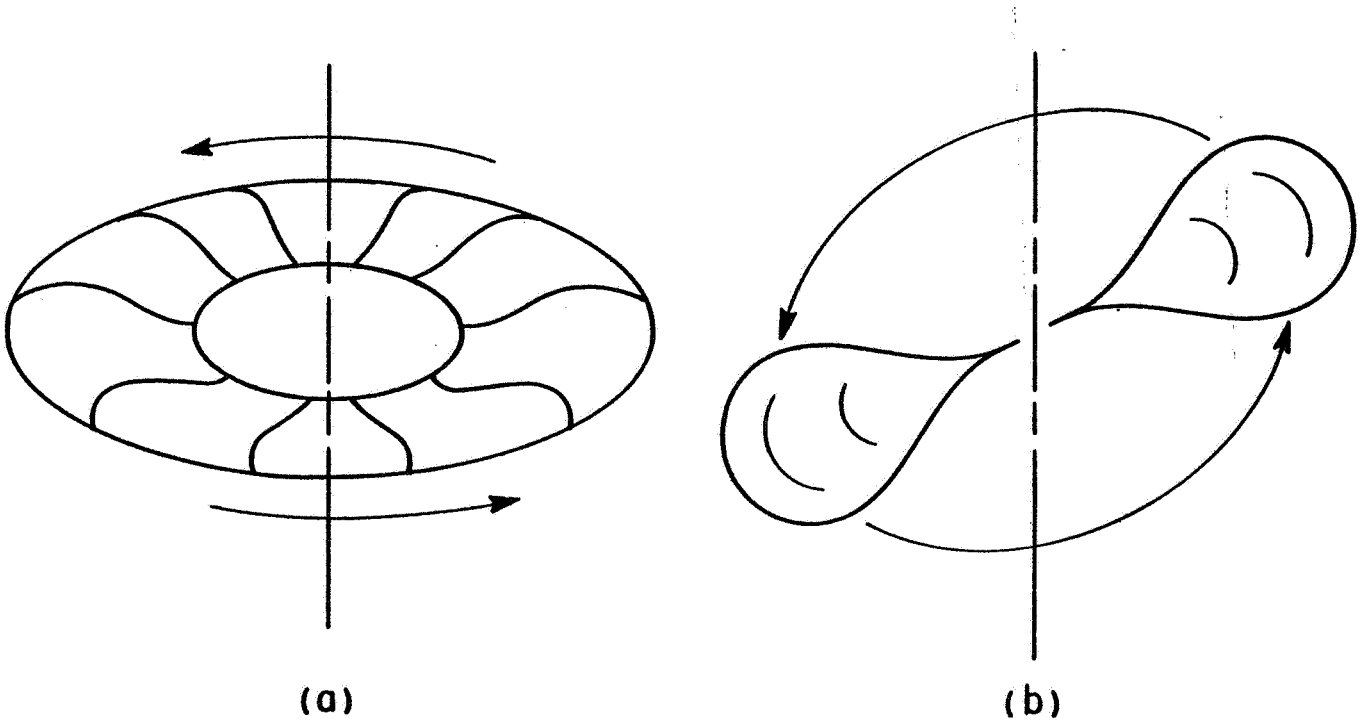

Fig. 9. Unstable shapes of a rotating liquid drop: (a) toroidal instability of Fig. 8, (b) dumb-bell instability observed in Skylab experiments.

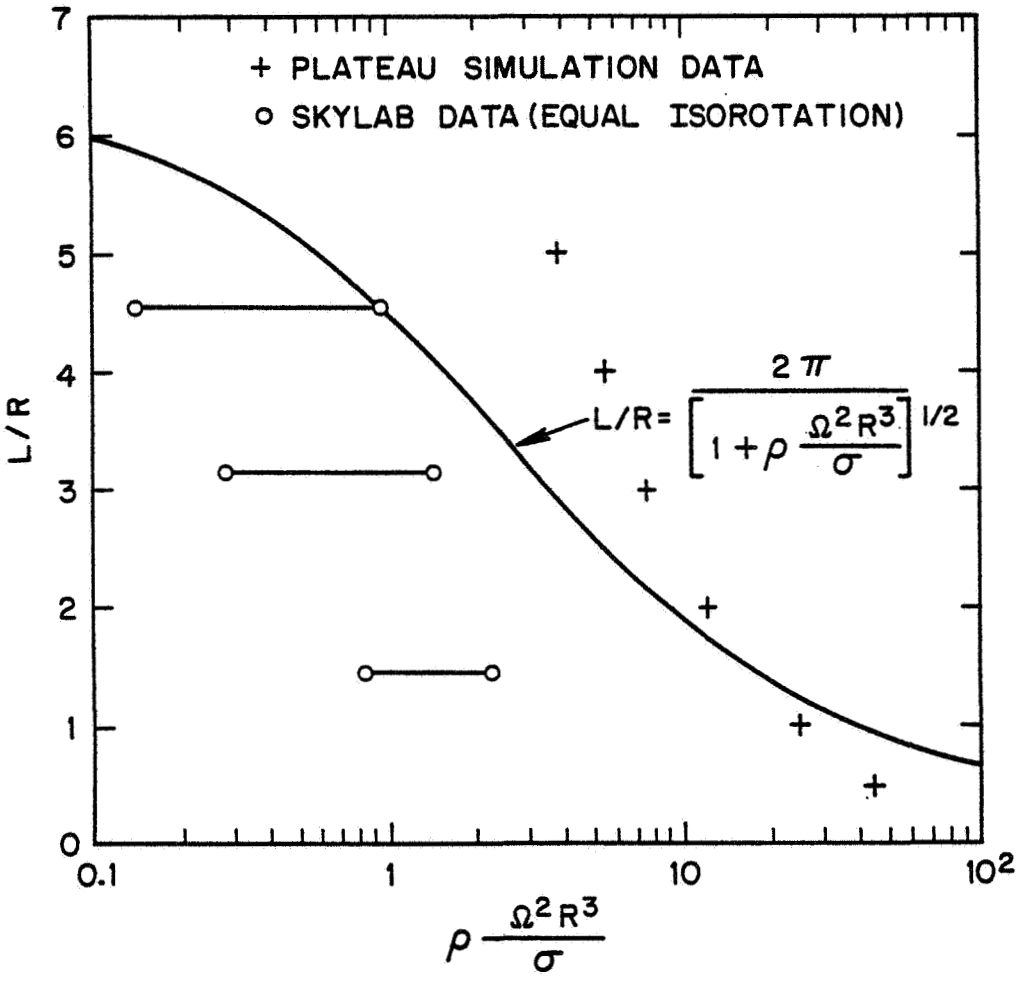

Fig. 10. Comparison of the rotational stability of cylindrical liquid zones in Plateau simulation and Skylab experiments with theory for axisymmetric modes.

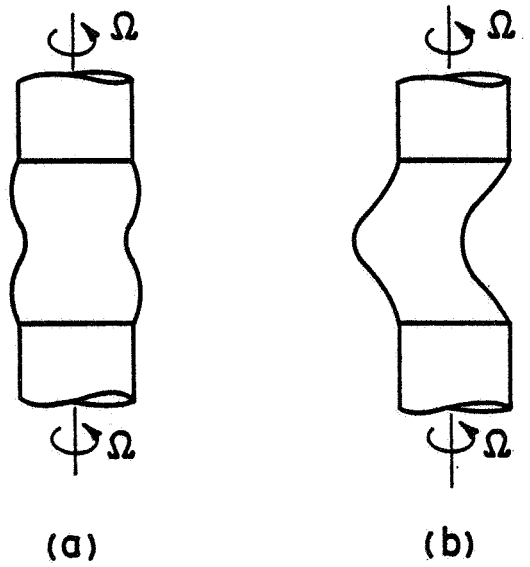

Fig. 11. Forms of rotating liquid zone surfaces: (a) axisymmetric mode observed in presence of highly viscous liquids, (b) nonaxisymmetric C-modes observed for water zones on Skylab.

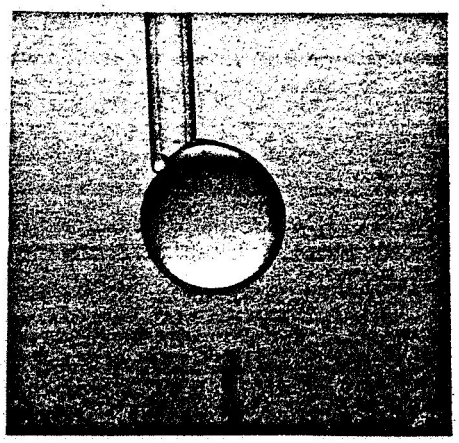

(a)

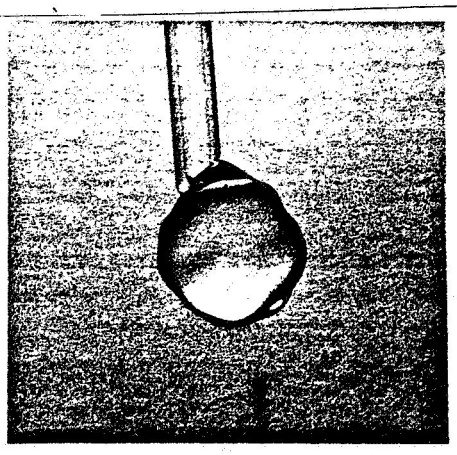

(b)

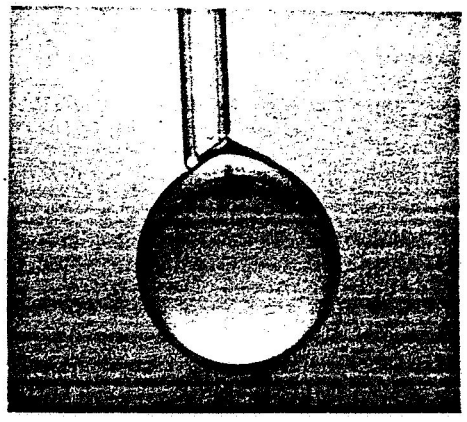

(c)

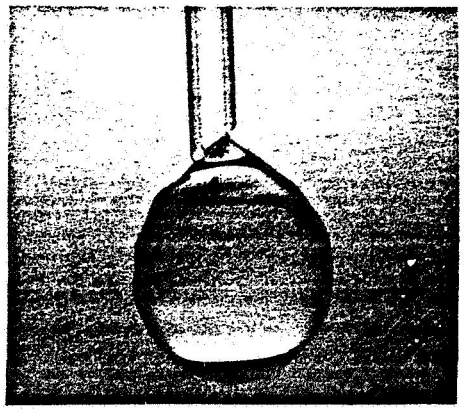

(d)

Fig. 12. Plateau simulation experiments using neutrally buoyant carbon tetrachloride plus benzene solution drops in water. (a) and (c) are static sessile drops, (b) and (d) are drops (a) and (c) respectively under vibrational conditions.

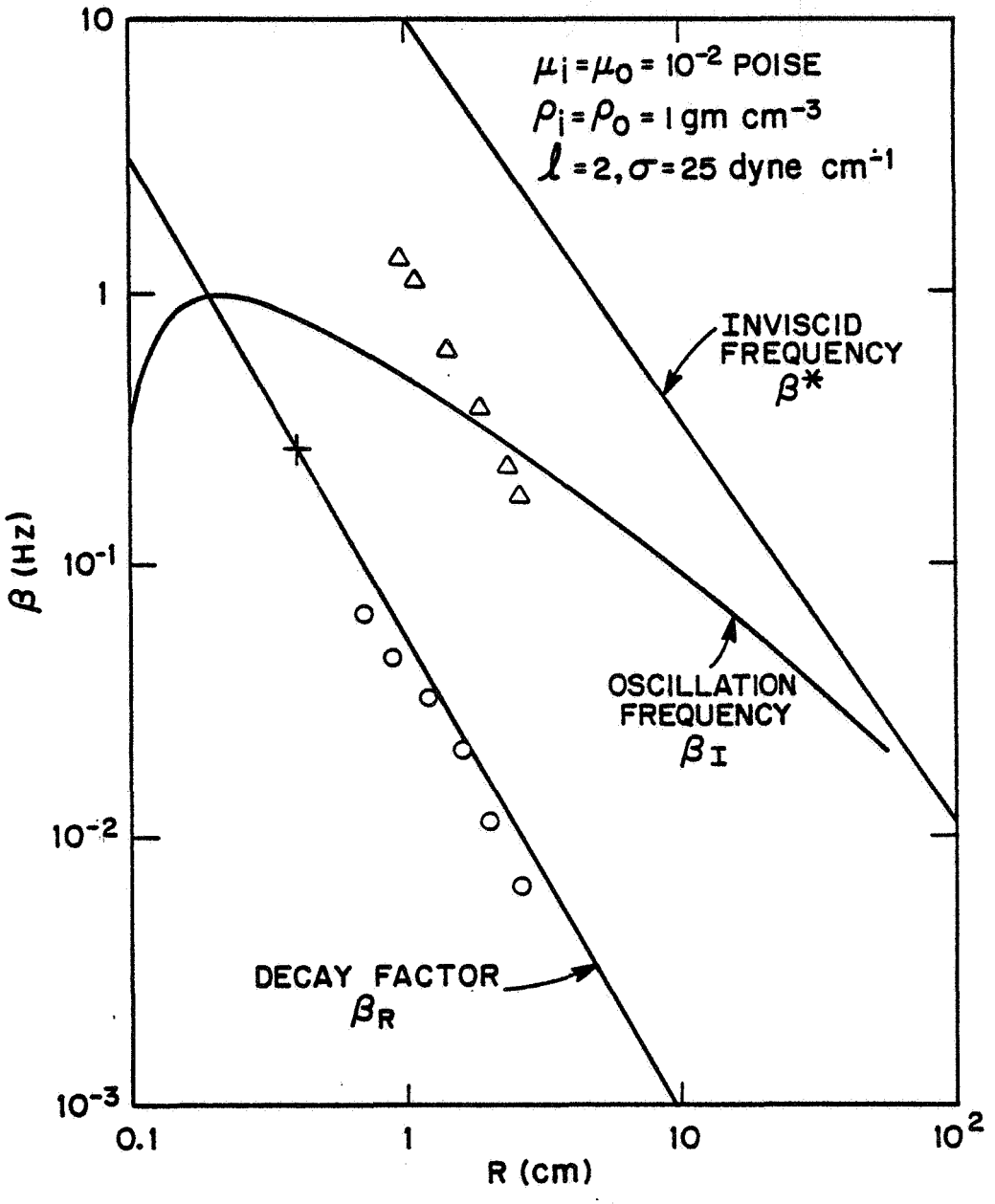

Fig. 13. Oscillation frequencies and decay rates of drops such as those in Fig. 12. Solid curves theoretically determined by Miller and Scriven.[27]

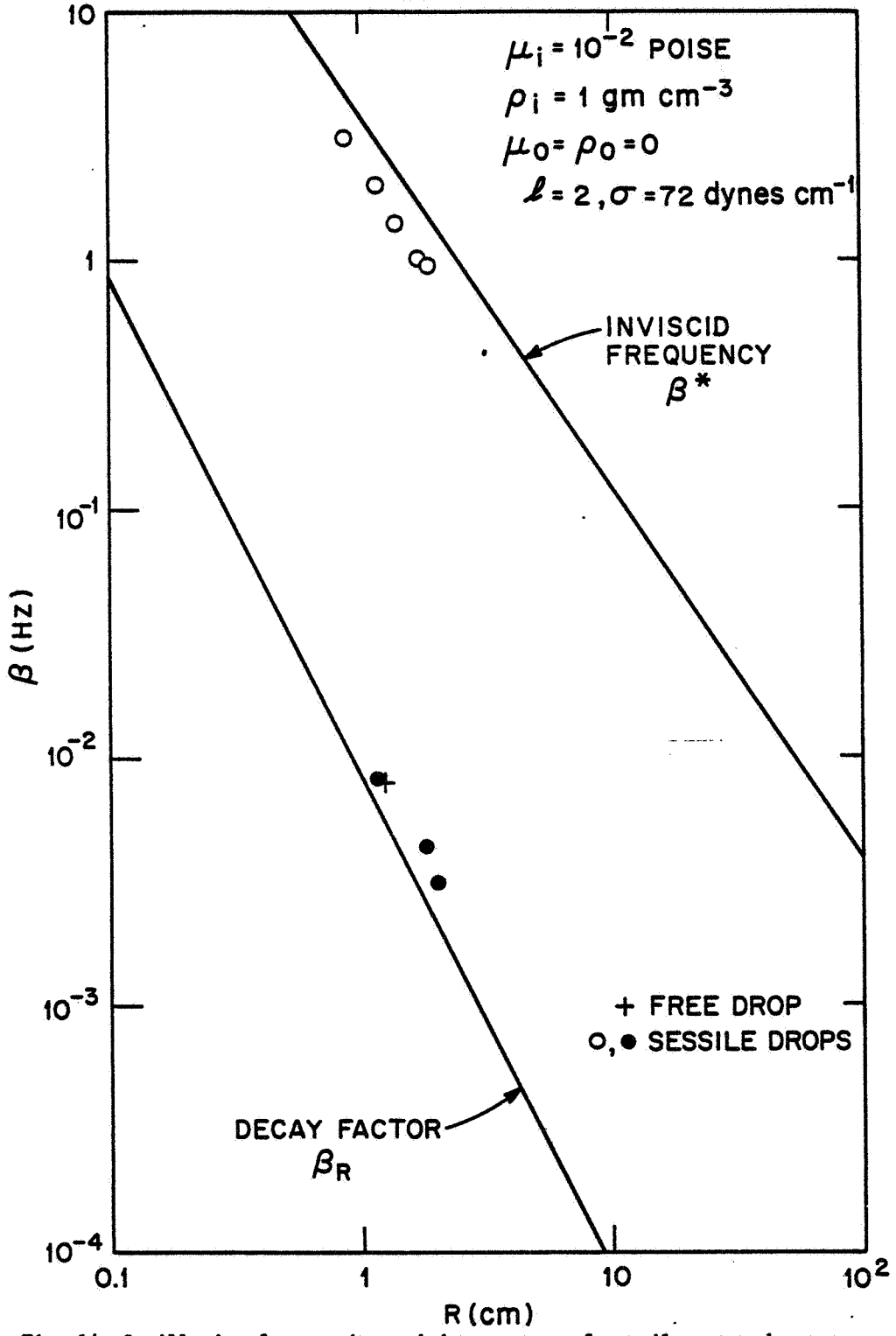

Fig. 14. Oscillation frequencies and decay rates of sessile water drops as measured from Skylab IV video-tape and compared to the theoretical solid curves of Miller and Scriven.(27)

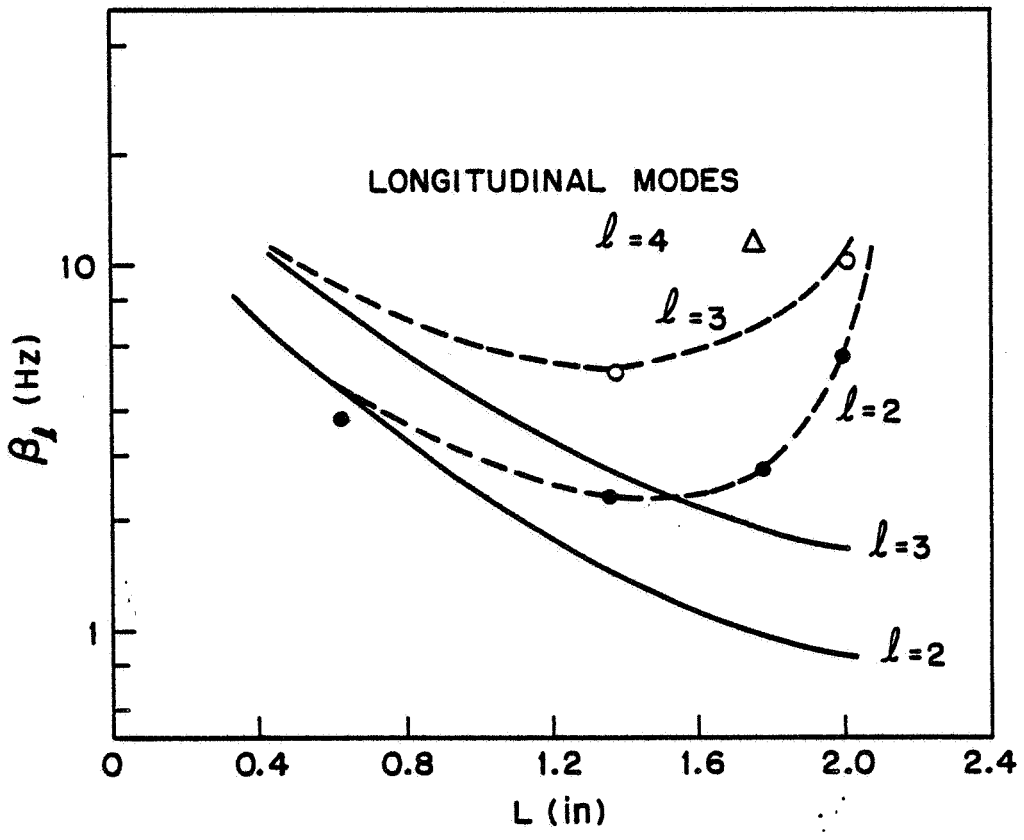

Fig. 15. Longitudinal oscillation frequencies of cylindrical liquid zones as measured from Skylab IV experiments as compared to the theoretical solid curves of Lamb.(26)